Electronic Supporting Information for

A family of fourteen soluble stable macrocyclic [$Ni^{II}_3Ln^{III}$] complexes

Humphrey L. C. Feltham, Sébastien Dhers, Mathieu Rouzières, Rodolphe Clérac, Annie K. Powell,* and Sally Brooker**

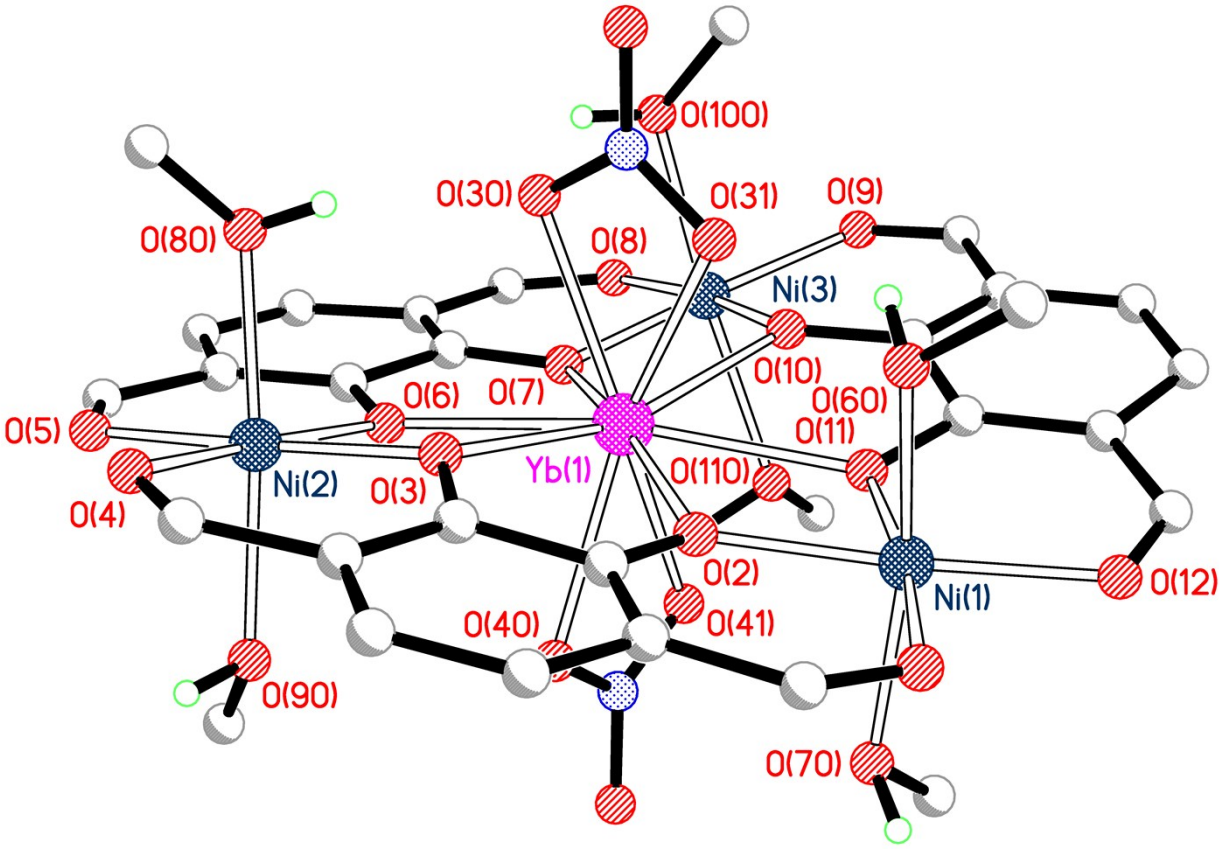

Figure S1. Perspective view of the crystal structure of $[Ni^{II}_3Yb^{III}(\mathbf{L^{Ald}})_3(NO_3)_2(MeOH)_{4.75}(H_2O)_{1.25}]^+$. For clarity, non-acidic hydrogen atoms and parts of the disordered atoms have been omitted. Selected bond lengths (Å): Yb(1)-O(2), 2.474(5); Yb(1)-O(3), 2.469(5); Yb(1)-O(6), 2.478(6); Yb(1)-O(7), 2.458(5); Yb(1)-O(10) 2.449(5); Yb(1)-O(11), 2.458(5); Yb(1)-O(30), 2.404(7); Yb(1)-O(31), 2.414(6); Yb(1)-O(40), 2.427(8); Yb(1)-O(41), 2.463(7); Ni(1)-O(1), 2.011(6); Ni(1)-O(2), 1.961(6); Ni(1)-O(11), 1.974(6); Ni(1)-O(12), 2.000(7); Ni(1)-O(60), 2.116(16); Ni(1)-O(61), 2.059(11); Ni(1)-O(70), 2.091(7); Ni(2)-O(3), 1.975(5); Ni(2)-O(4), 2.005(6); Ni(2)-O(5), 2.011(6); Ni(2)-O(6), 1.974(6); Ni(2)-O(80), 2.059(8); Ni(2)-O(81), 2.08(3); Ni(2)-O(90), 2.086(8) Ni(3)-O(7), 1.964(5); Ni(3)-O(8), 2.010(7); Ni(3)-O(9), 2.003(6); Ni(3)-O(10), 1.982(5) Ni(3)-O(100), 2.055(7); Ni(3)-O(110), 2.237(15); Ni(3)-O(111), 1.983(16). Selected angles (°): Ni(1)-O(2)-Yb(1), 111.0(2); Ni(1)-O(11)-Yb(1), 111.2(2); Ni(2)-O(3)-Yb(1), 110.5(2); Ni(2)-O(6)-Yb(1), 110.2(2); Ni(3)-O(7)-Yb(1), 111.0(2); Ni(3)-O(10)-Yb(1), 110.7(2).

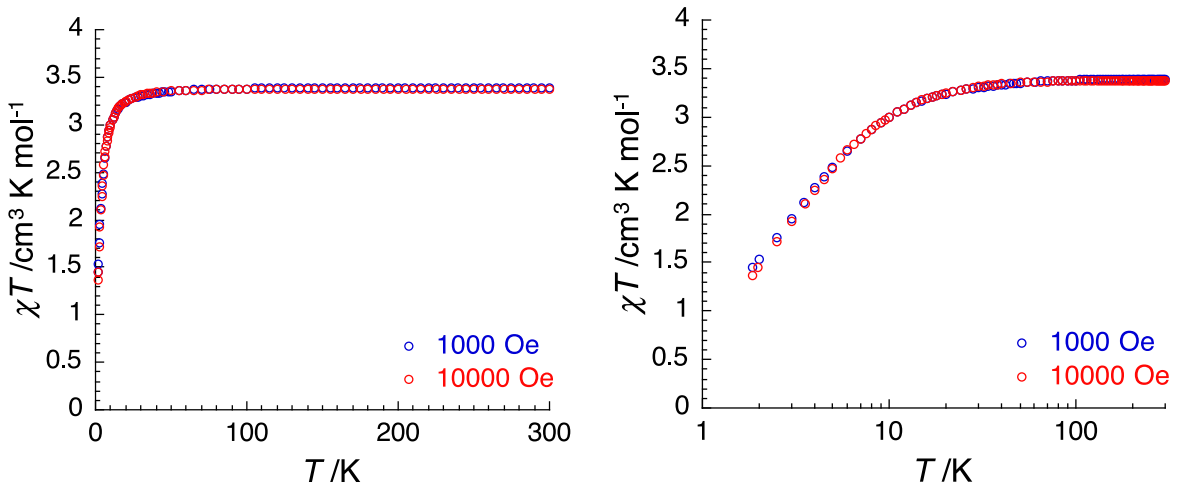

Figure S2. Temperature dependence of the χT product for $[Ni^{II}_3La^{III}(\mathbf{L^{Pr}})]$ (with χ defined as the molar magnetic susceptibility at 1000 Oe and equal to M/H per mole of complex).

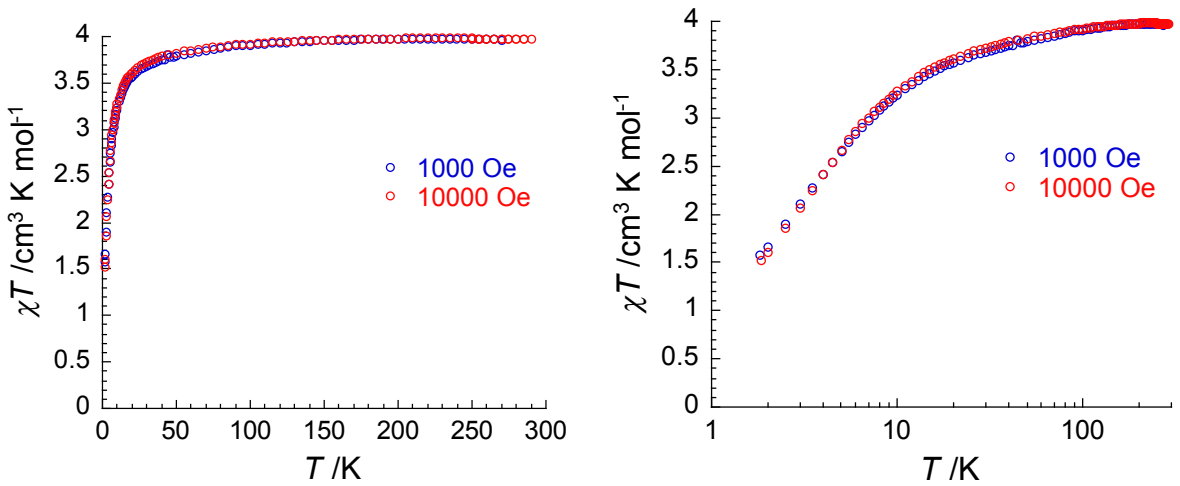

Figure S3. Temperature dependence of the χT product for $[Ni^{II}_3Ce^{III}(\mathbf{L^{Pr}})]$ (with χ defined as the molar magnetic susceptibility at 1000 Oe and equal to M/H per mole of complex).

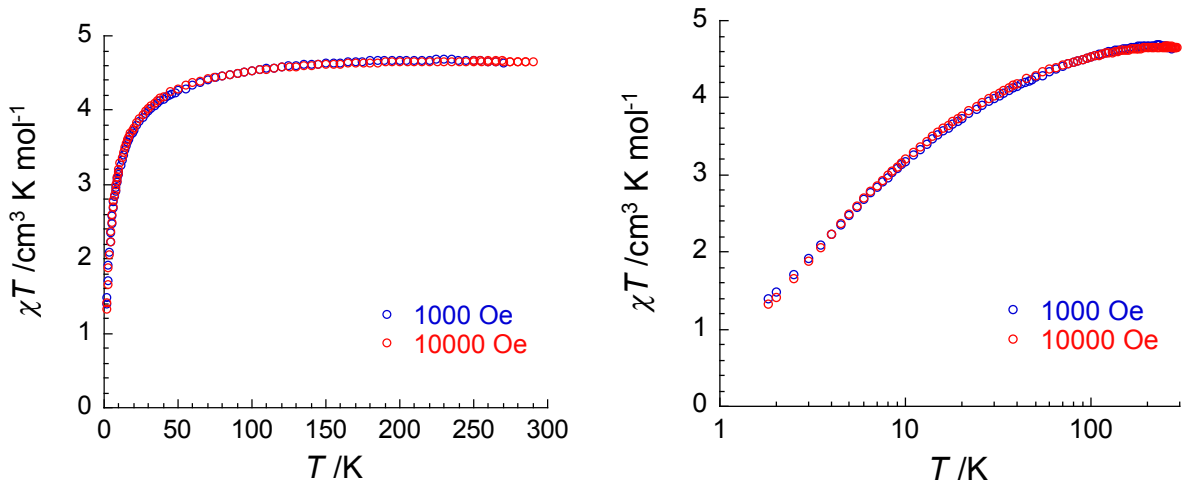

Figure S4. Temperature dependence of the χT product for $[Ni^{II}_3Pr^{III}(\mathbf{L^{Pr}})]$ (with χ defined as the molar magnetic susceptibility at 1000 Oe and equal to M/H per mole of complex).

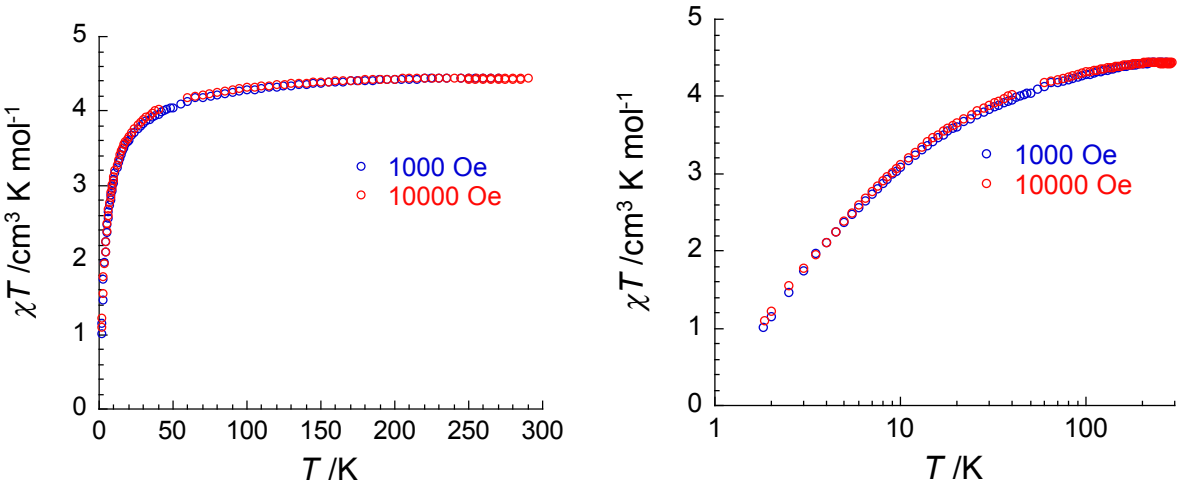

Figure S5. Temperature dependence of the χT product for $[Ni^{II}_3Nd^{III}(\mathbf{L^{Pr}})]$ (with χ defined as the molar magnetic susceptibility at 1000 Oe and equal to M/H per mole of complex).

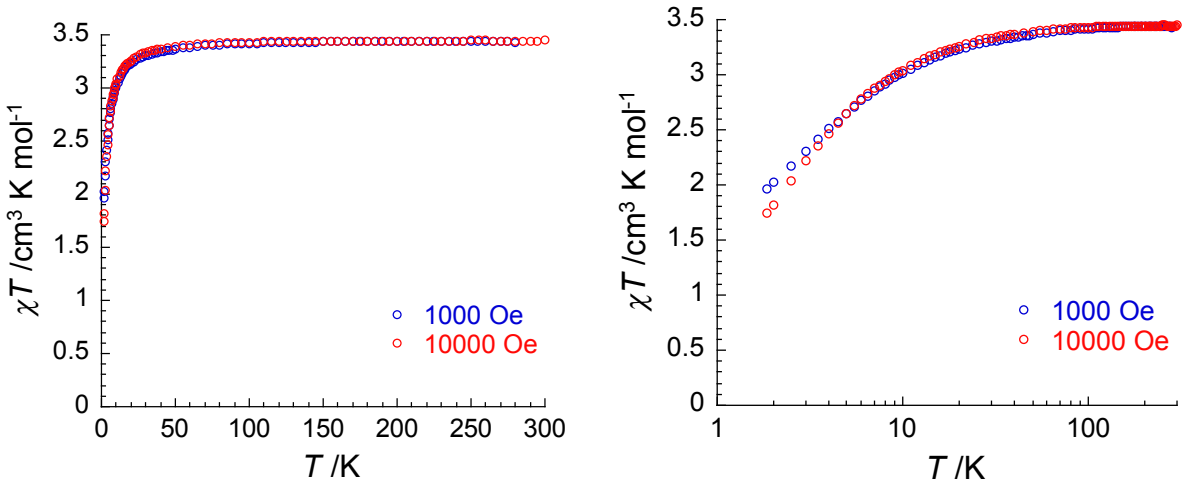

Figure S6. Temperature dependence of the χT product for $[Ni^{II}_3Sm^{III}(\mathbf{L^{Pr}})]$ (with χ defined as the molar magnetic susceptibility at 1000 Oe and equal to M/H per mole of complex).

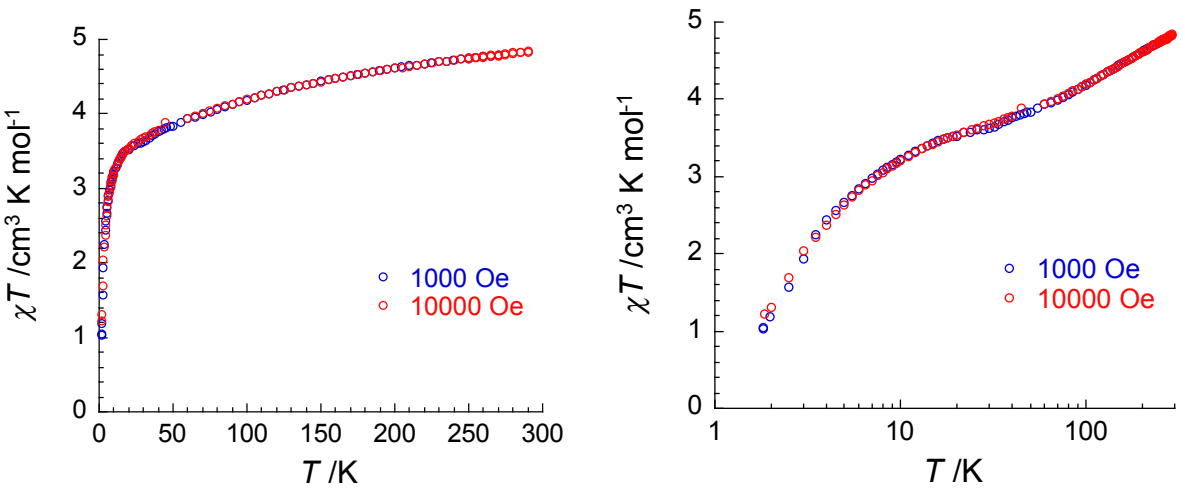

Figure S7. Temperature dependence of the χT product for $[Ni^{II}_3Eu^{III}(\mathbf{L^{Pr}})]$ (with χ defined as the molar magnetic susceptibility at 1000 Oe and equal to M/H per mole of complex).

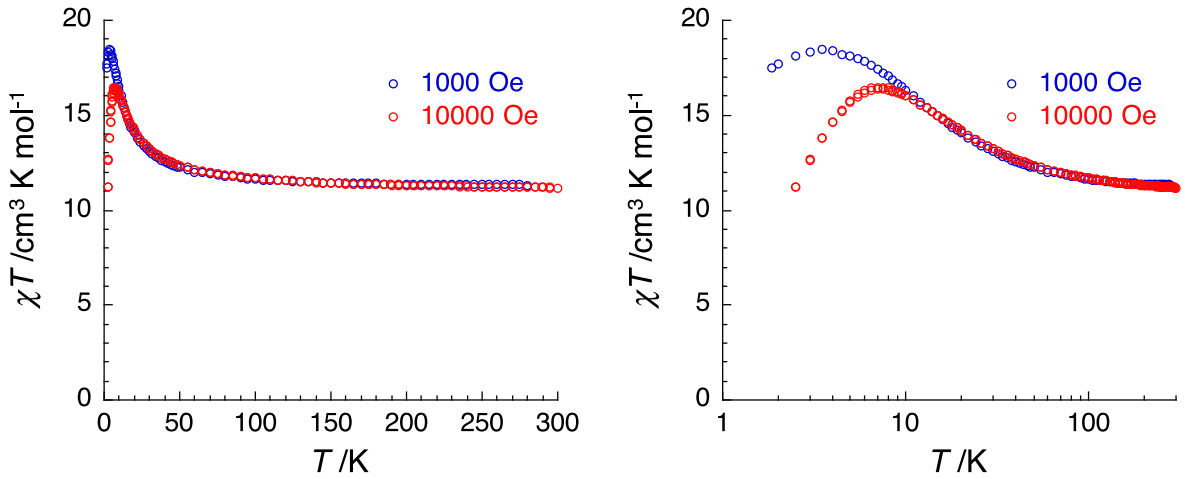

Figure S8. Temperature dependence of the χT product for $[Ni^{II}_3Gd^{III}(\mathbf{L^{Pr}})]$ (with χ defined as the molar magnetic susceptibility at 1000 Oe and equal to M/H per mole of complex).

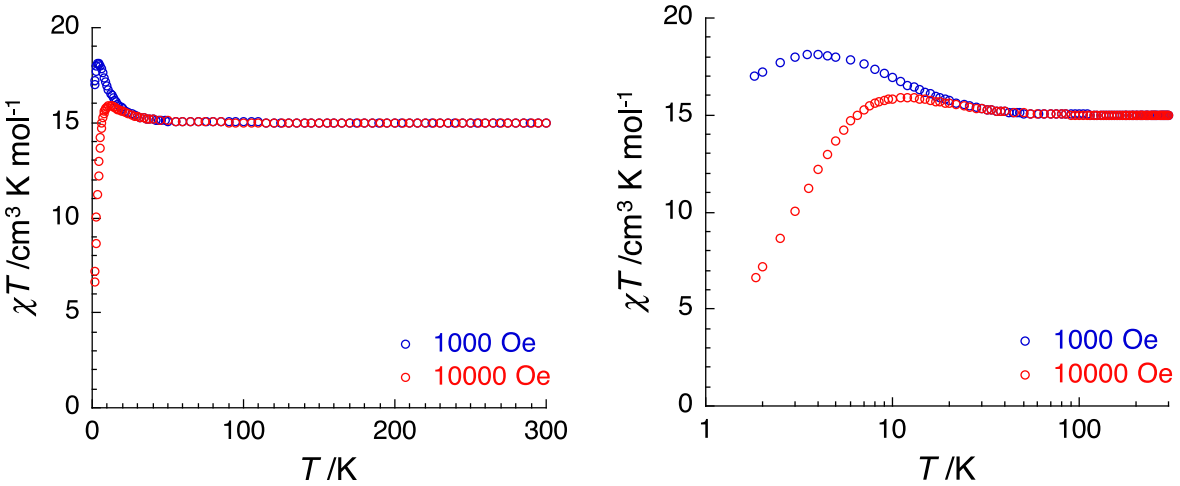

Figure S9. Temperature dependence of the χT product for $[Ni^{II}_3Tb^{III}(\mathbf{L^{Pr}})]$ (with χ defined as the molar magnetic susceptibility at 1000 Oe and equal to M/H per mole of complex).

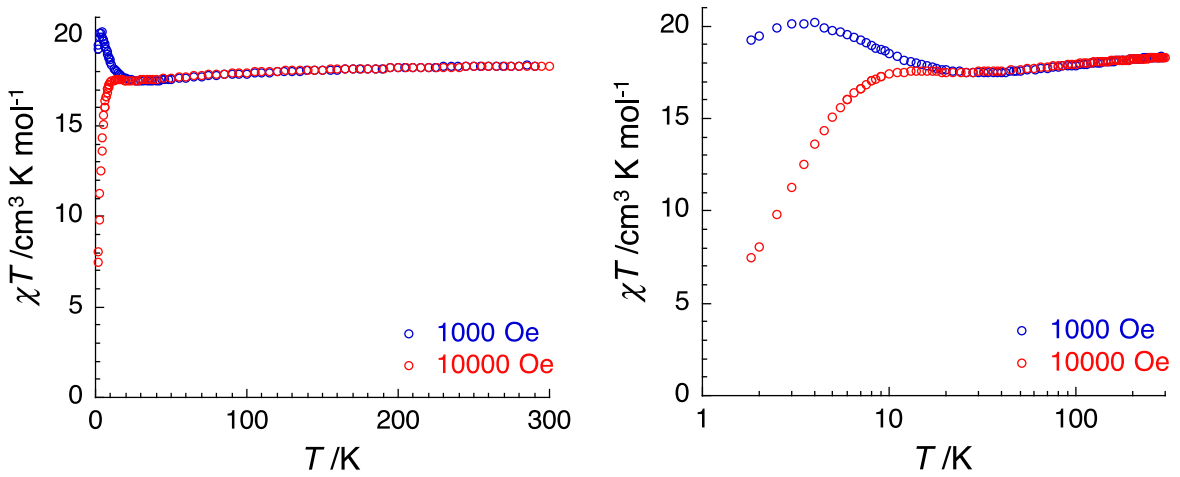

Figure S10. Temperature dependence of the χT product for $[Ni^{II}_3Dy^{III}(\mathbf{L^{Pr}})]$ (with χ defined as the molar magnetic susceptibility at 1000 Oe and equal to M/H per mole of complex).

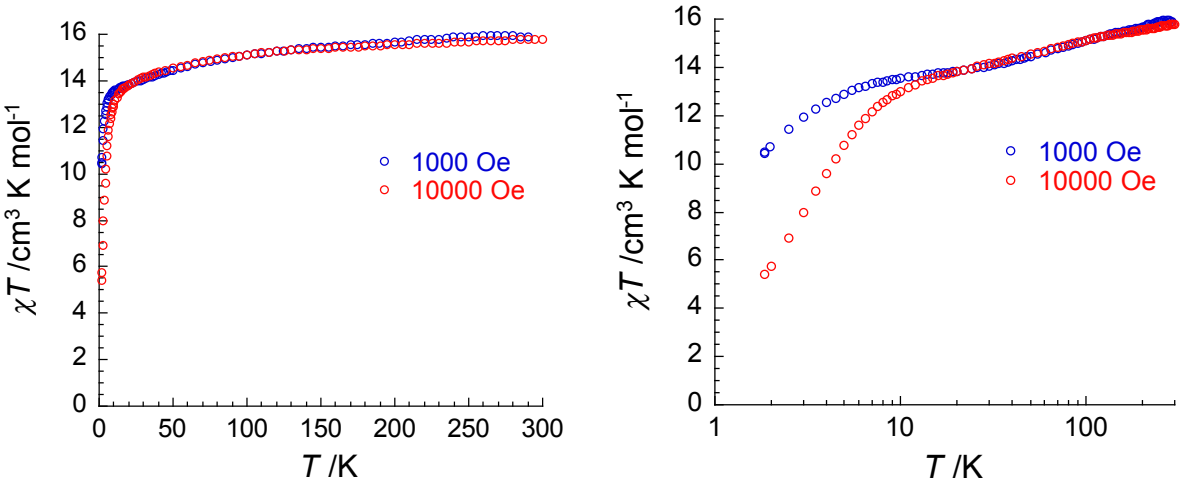

Figure S11. Temperature dependence of the χT product for $[Ni^{II}_3Ho^{III}(\mathbf{L^{Pr}})]$ (with χ defined as the molar magnetic susceptibility at 1000 Oe and equal to M/H per mole of complex).

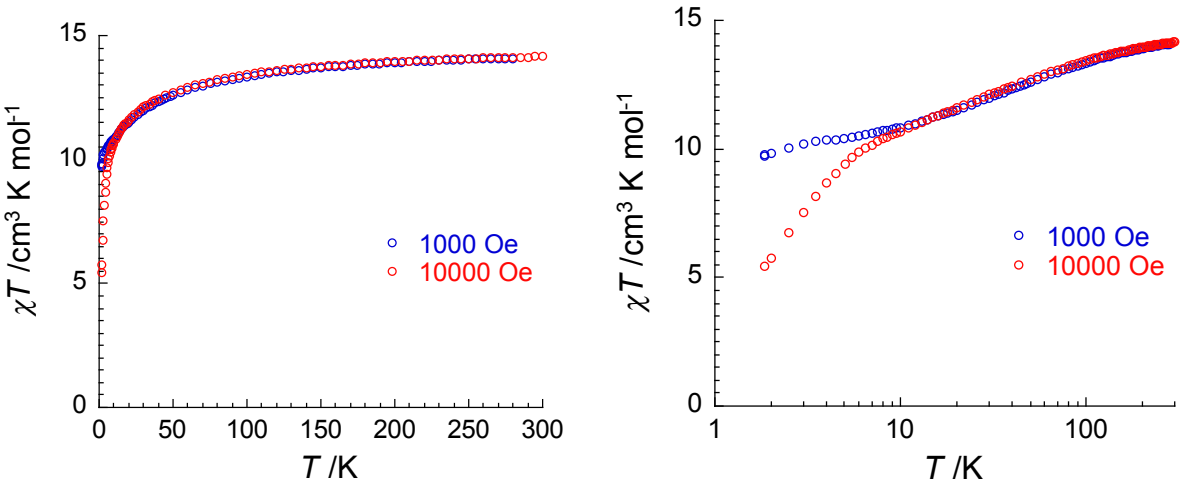

Figure S12. Temperature dependence of the χT product for $[Ni^{II}_3Er^{III}(\mathbf{L^{Pr}})]$ (with χ defined as the molar magnetic susceptibility at 1000 Oe and equal to M/H per mole of complex).

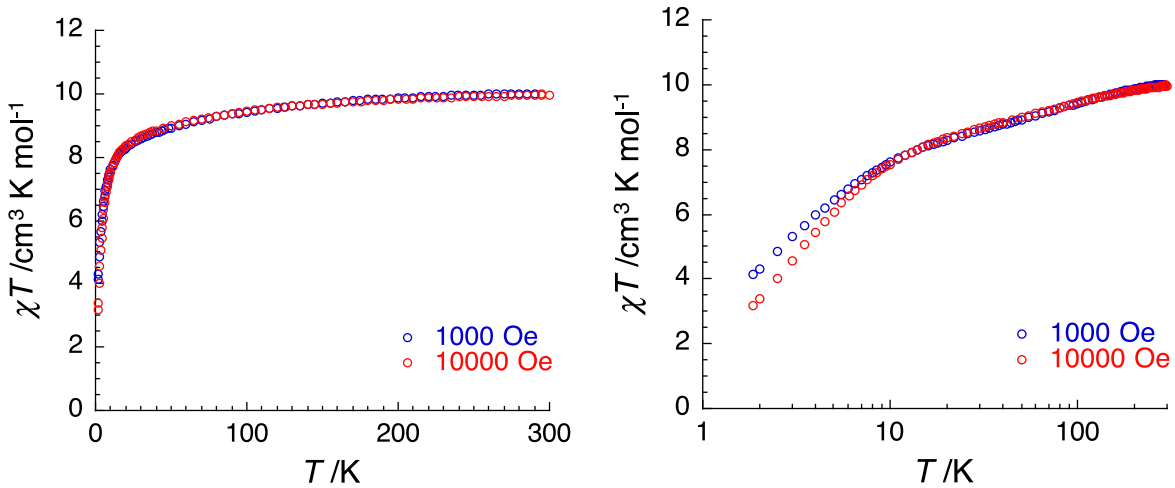

Figure S13. Temperature dependence of the χT product for $[Ni^{II}_3Tm^{III}(\mathbf{L^{Pr}})]$ (with χ defined as the molar magnetic susceptibility at 1000 Oe and equal to M/H per mole of complex).

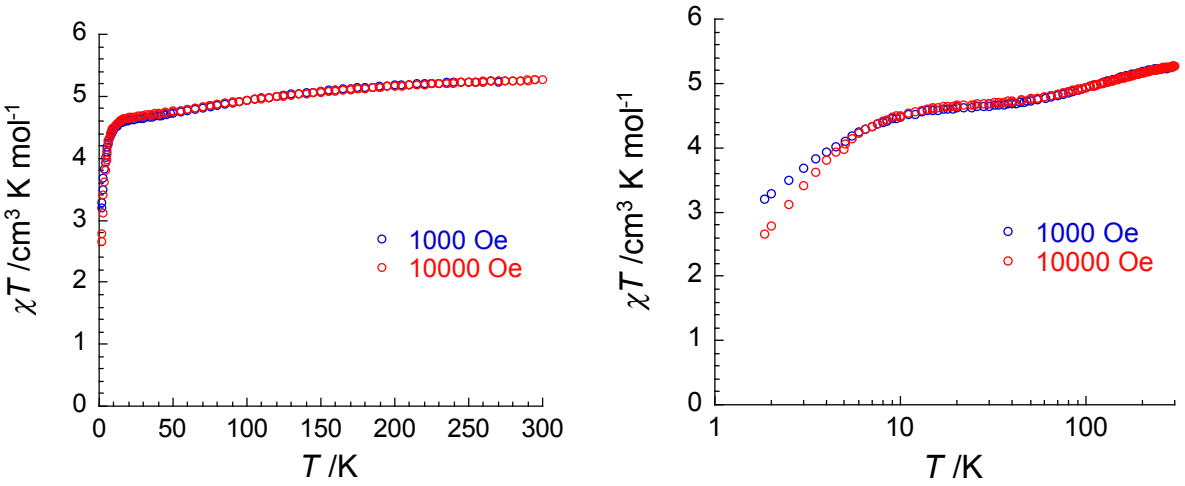

Figure S14. Temperature dependence of the χT product for $[Ni^{II}_3Yb^{III}(\mathbf{L^{Pr}})]$ (with χ defined as the molar magnetic susceptibility at 1000 Oe and equal to M/H per mole of complex).

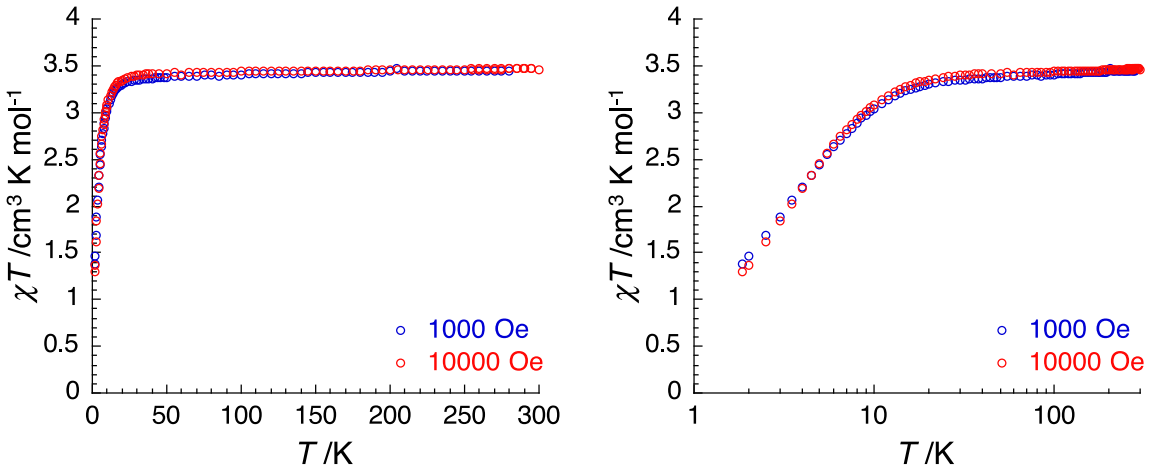

Figure S15. Temperature dependence of the χT product for $[Ni^{II}_3Lu^{III}(\mathbf{L^{Pr}})]$ (with χ defined as the molar magnetic susceptibility at 1000 Oe and equal to M/H per mole of complex).

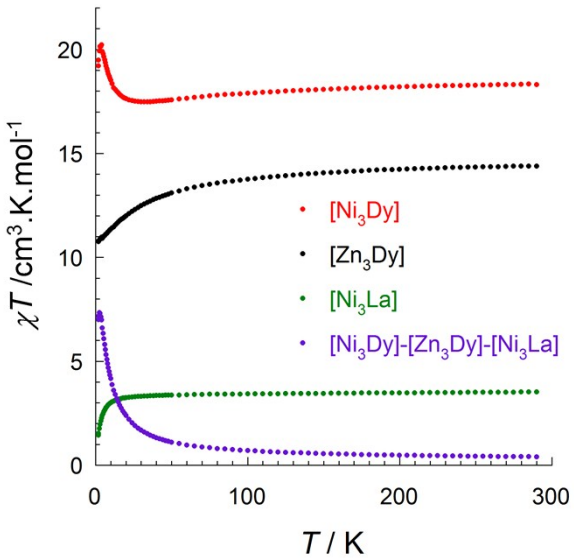

Figure S16. Temperature dependence of the χT product in a 1000 Oe dc field (with χ defined as the molar magnetic susceptibility at 1000 Oe and equal to M/H per mole of complex) for $[Ni^{II}_3La^{III}(\mathbf{L^{Pr}})]$, $[Zn^{II}_3Dy^{III}(\mathbf{L^{Pr}})]$, $[Ni^{II}_3Dy^{III}(\mathbf{L^{Pr}})]$ and the remainder after subtraction of the two analogues.

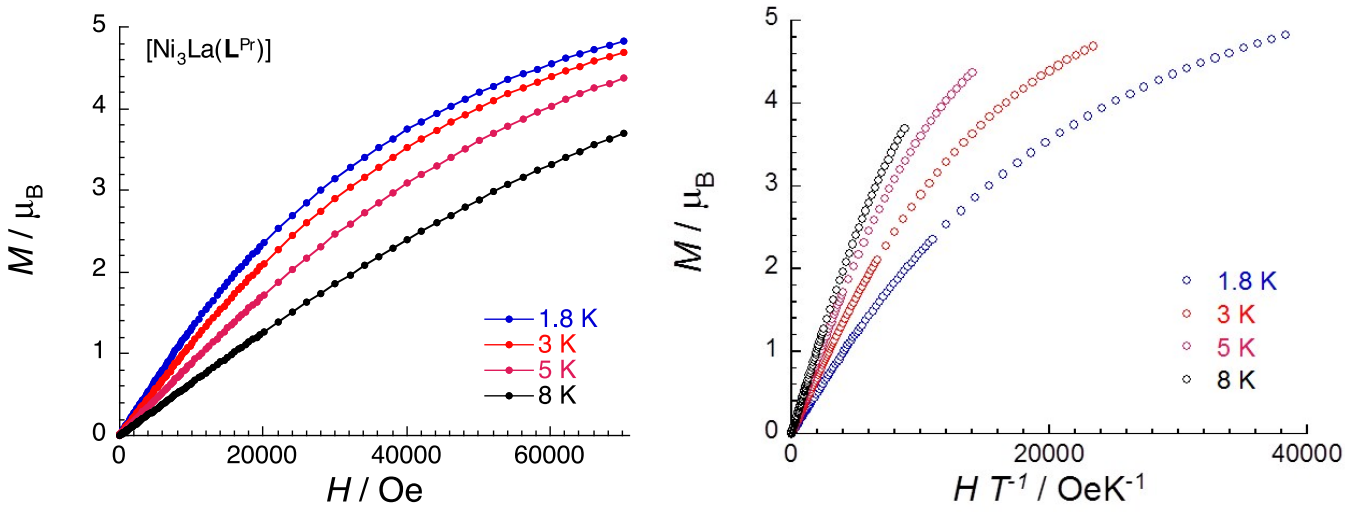

Figure S17. (Left) Field dependence of magnetisation for [$Ni^{II}_3La^{III}$(**L^{Pr}**)] at the temperatures indicated, scanning at 100 – 200 Oe.min^{-1}. (Right) Field dependence of reduced magnetisation at the temperatures indicated.

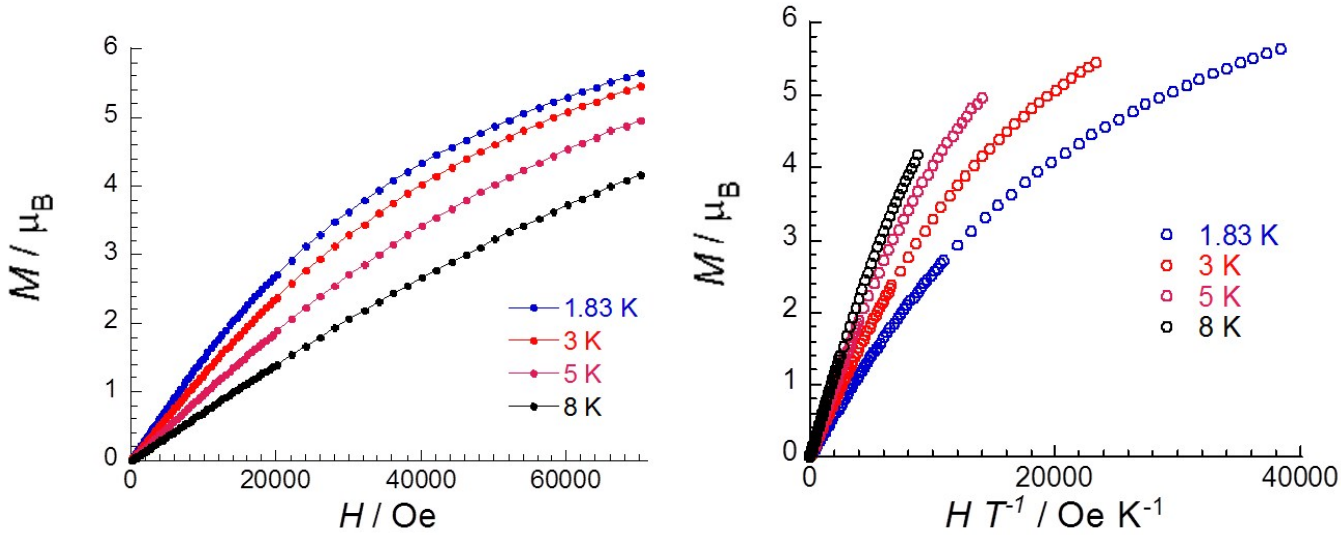

Figure S18. (Left) Field dependence of magnetisation for [$Ni^{II}_3Ce^{III}$(**L^{Pr}**)] at the temperatures indicated, scanning at 100 – 200 Oe.min^{-1}. (Right) Field dependence of reduced magnetisation at the temperatures indicated.

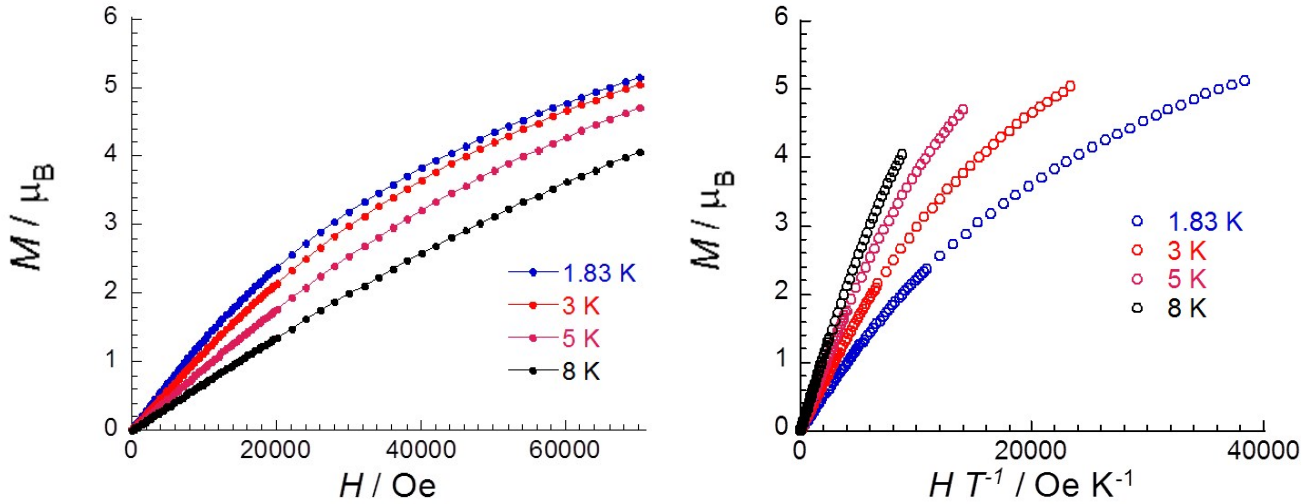

Figure S19. (Left) Field dependence of magnetisation for [$Ni^{II}_3Pr^{III}$(**L^{Pr}**)] at the temperatures indicated, scanning at 100 – 200 Oe.min^{-1}. (Right) Field dependence of reduced magnetisation at the temperatures indicated.

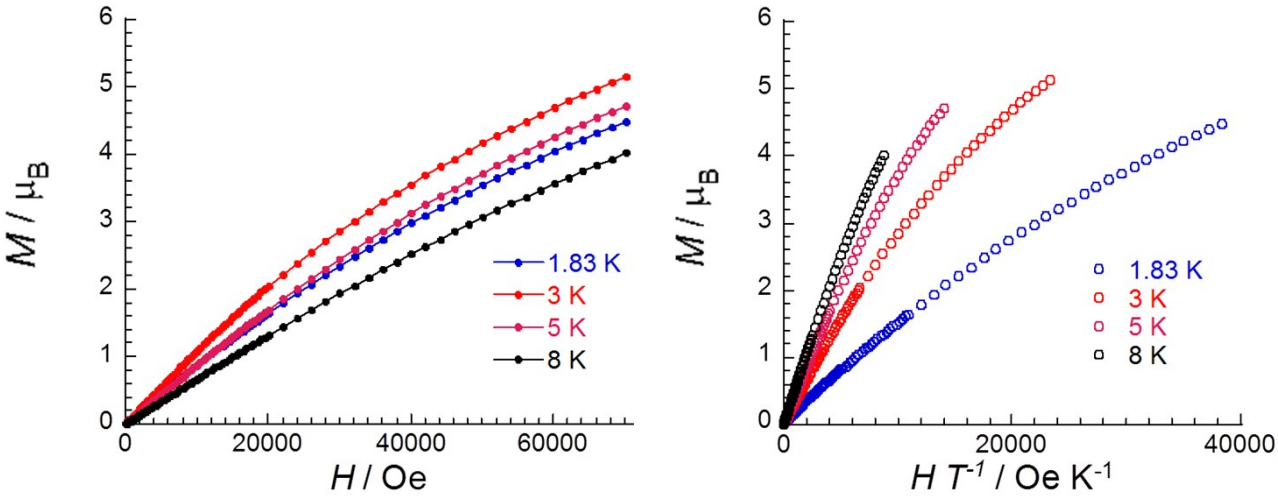

Figure S20. (Left) Field dependence of magnetisation for [$Ni^{II}_3Nd^{III}$(**L**^{Pr})] at the temperatures indicated, scanning at 100 – 200 Oe.min^{-1}. (Right) Field dependence of reduced magnetisation at the temperatures indicated.

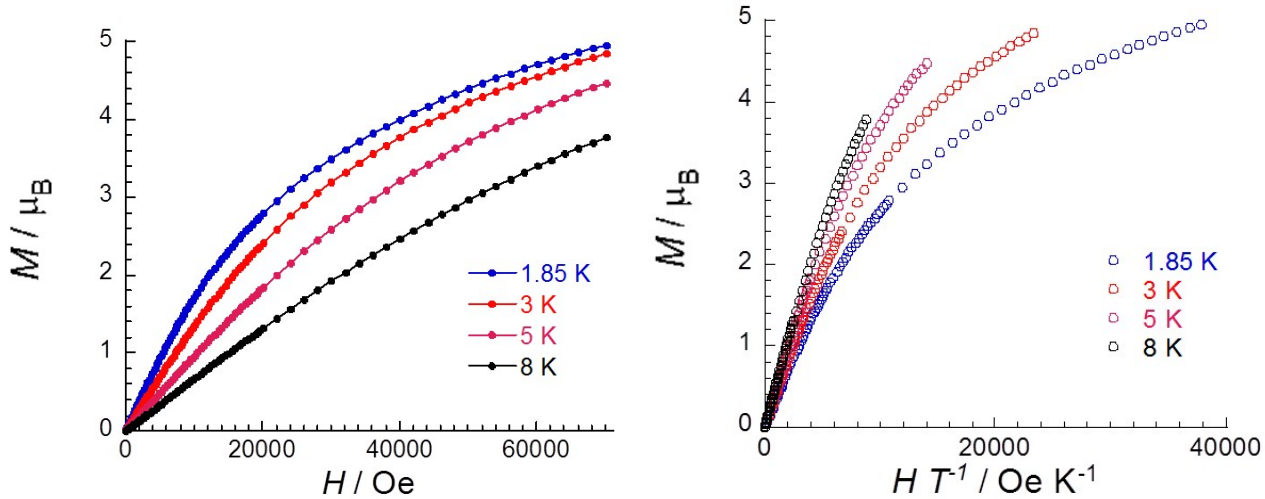

Figure S21. (Left) Field dependence of magnetisation for [$Ni^{II}_3Sm^{III}$(**L**^{Pr})] at the temperatures indicated, scanning at 100 – 200 Oe.min^{-1}. (Right) Field dependence of reduced magnetisation at the temperatures indicated.

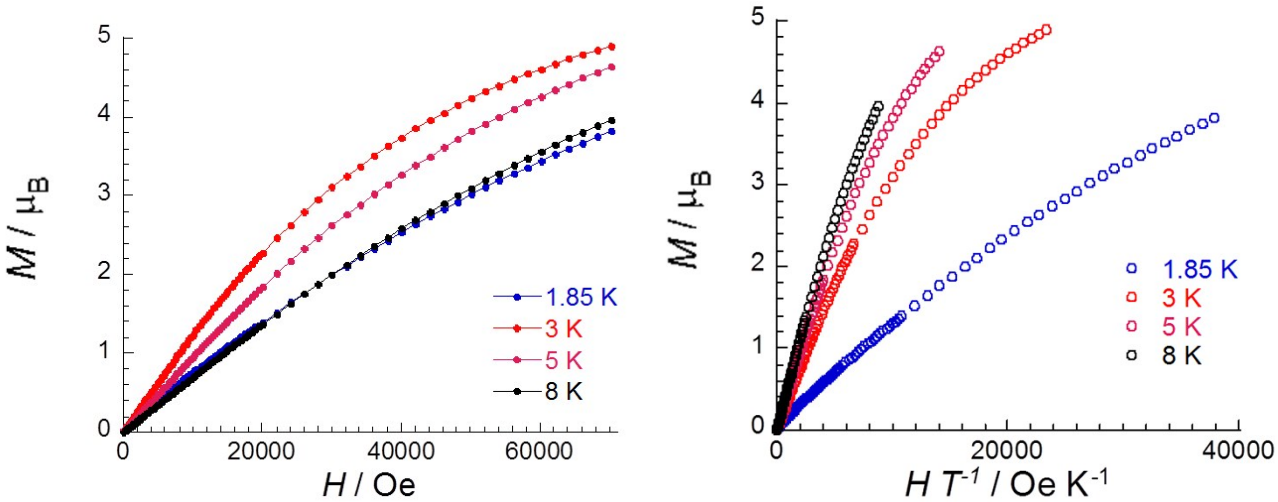

Figure S22. (Left) Field dependence of magnetisation for [$Ni^{II}_3Eu^{III}$(**L**^{Pr})] at the temperatures indicated, scanning at 100 – 200 Oe.min^{-1}. (Right) Field dependence of reduced magnetisation at the temperatures indicated.

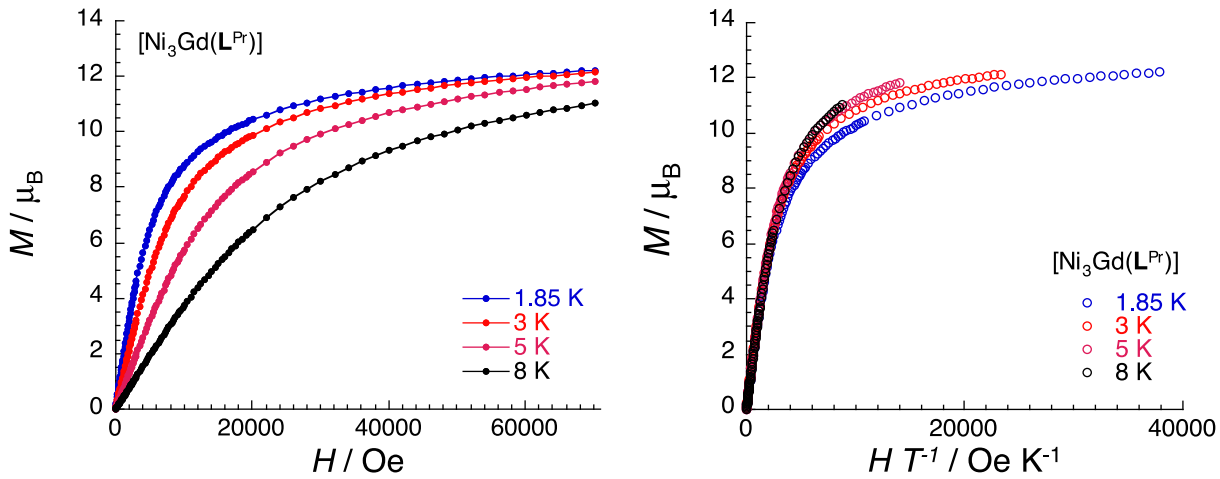

Figure S23. (Left) Field dependence of magnetisation for $[Ni^{II}_3Gd^{III}(\mathbf{L^{Pr}})]$ at the temperatures indicated, scanning at 100 – 200 Oe.min^{-1}. (Right) Field dependence of reduced magnetisation at the temperatures indicated.

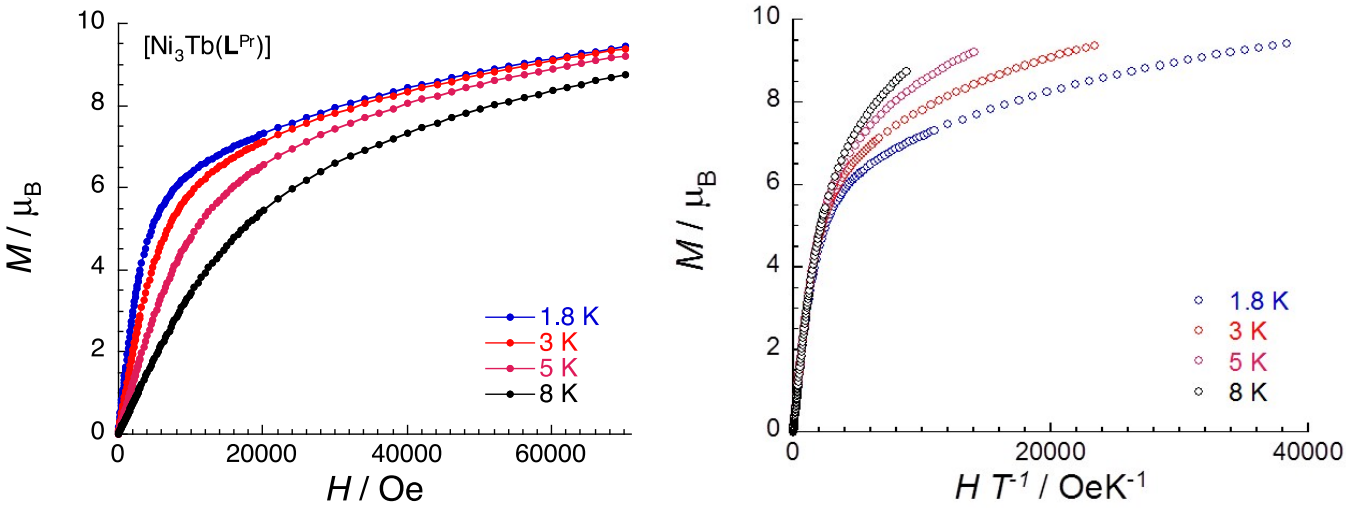

Figure S24. (Left) Field dependence of magnetisation for $[Ni^{II}_3Tb^{III}(\mathbf{L^{Pr}})]$ at the temperatures indicated, scanning at 100 – 200 Oe.min^{-1}. (Right) Field dependence of reduced magnetisation at the temperatures indicated.

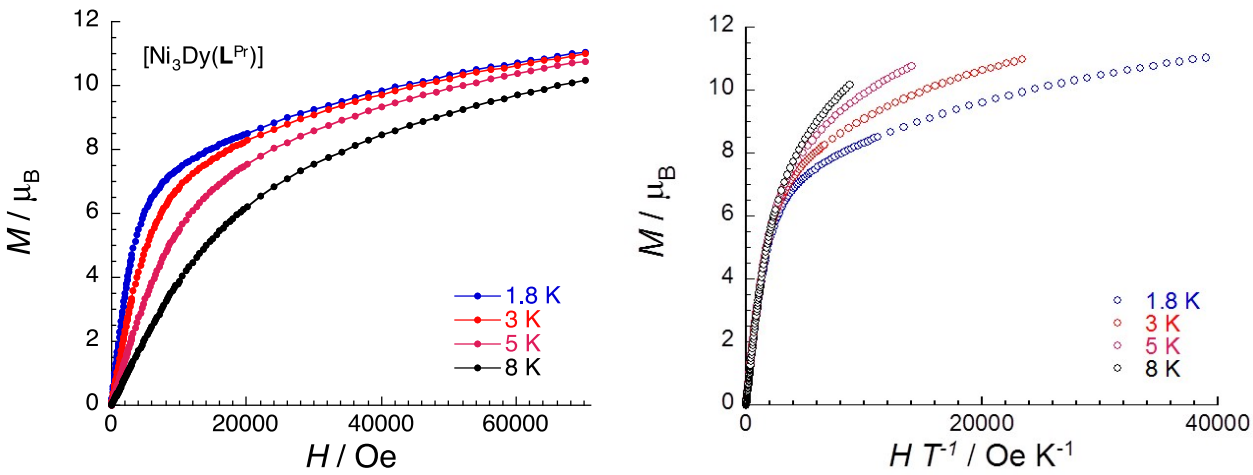

Figure S25. (Left) Field dependence of magnetisation for $[Ni^{II}_3Dy^{III}(\mathbf{L^{Pr}})]$ at the temperatures indicated, scanning at 100 – 200 Oe.min^{-1}. (Right) Field dependence of reduced magnetisation at the temperatures indicated.

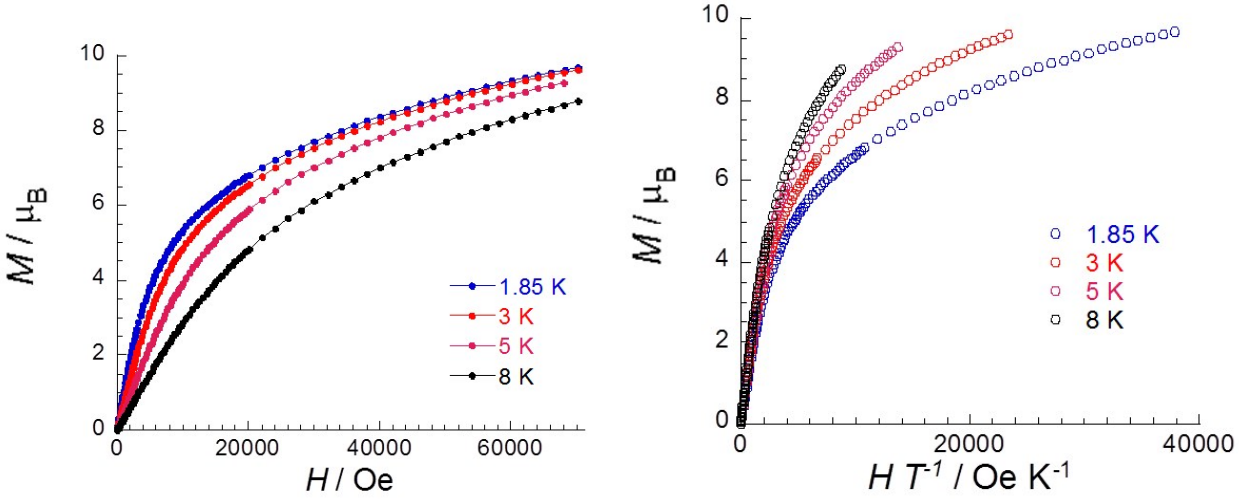

Figure S26. (Left) Field dependence of magnetisation for [$Ni^{II}_3Ho^{III}$(**L**^{Pr})] at the temperatures indicated, scanning at 100 – 200 Oe.min^{-1}. (Right) Field dependence of reduced magnetisation at the temperatures indicated.

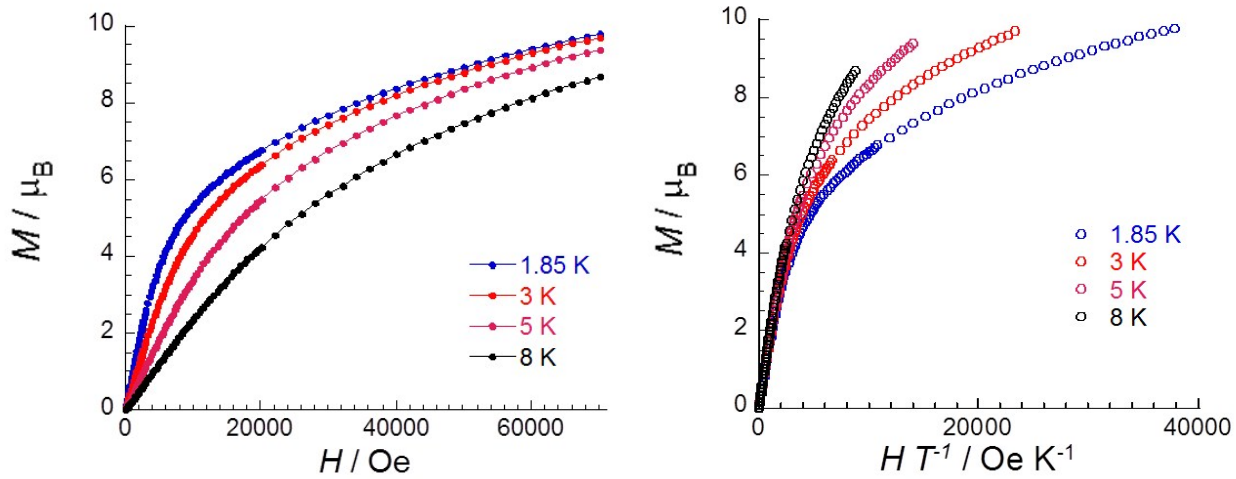

Figure S27. (Left) Field dependence of magnetisation for [$Ni^{II}_3Er^{III}$(**L**^{Pr})] at the temperatures indicated, scanning at 100 – 200 Oe.min^{-1}. (Right) Field dependence of reduced magnetisation at the temperatures indicated.

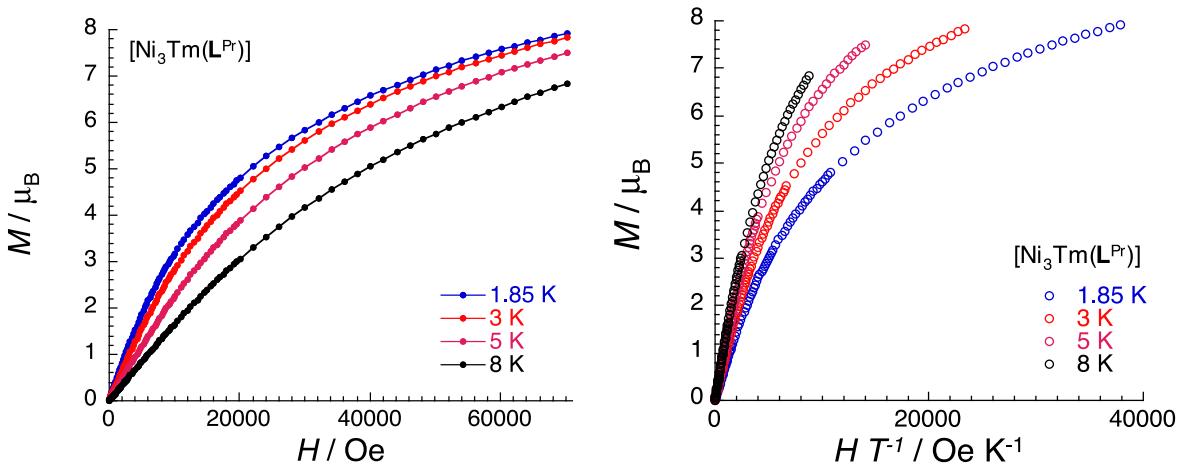

Figure S28. (Left) Field dependence of magnetisation for [$Ni^{II}_3Tm^{III}$(**L**^{Pr})] at the temperatures indicated, scanning at 100 – 200 Oe.min^{-1}. (Right) Field dependence of reduced magnetisation at the temperatures indicated.

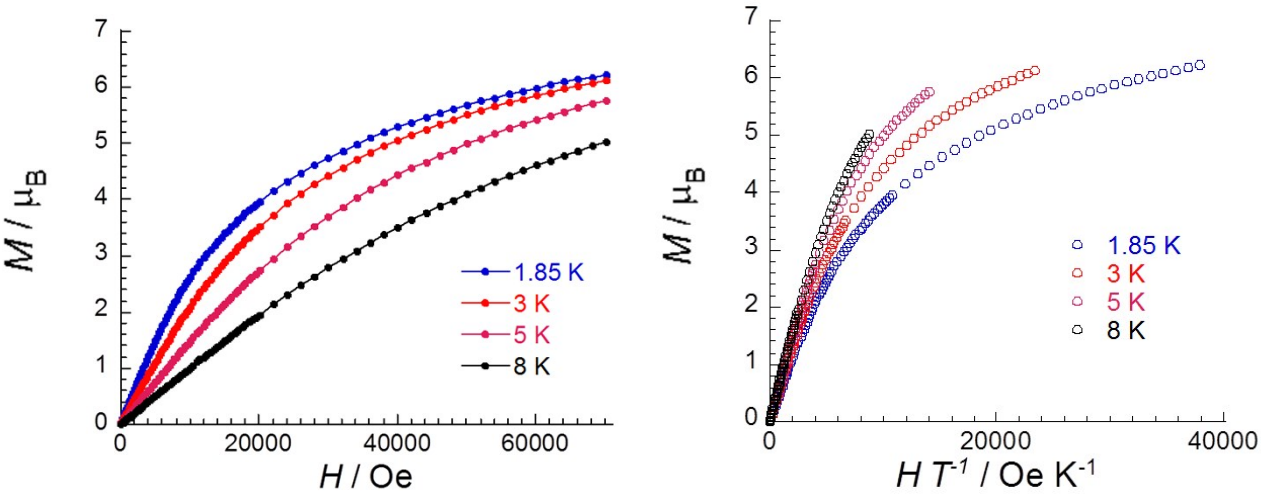

Figure S29. (Left) Field dependence of magnetisation for $[Ni^{II}_3Yb^{III}(\mathbf{L^{Pr}})]$ at the temperatures indicated, scanning at 100 – 200 Oe.min^{-1}. (Right) Field dependence of reduced magnetisation at the temperatures indicated.

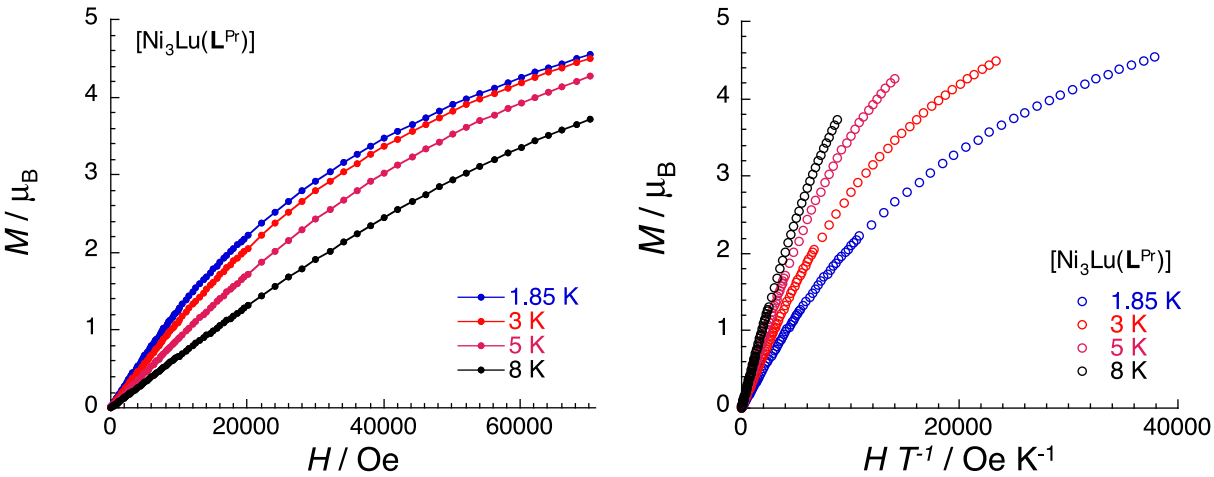

Figure S30. (Left) Field dependence of magnetisation for $[Ni^{II}_3Lu^{III}(\mathbf{L^{Pr}})]$ at the temperatures indicated, scanning at 100 – 200 Oe.min^{-1}. (Right) Field dependence of reduced magnetisation at the temperatures indicated.

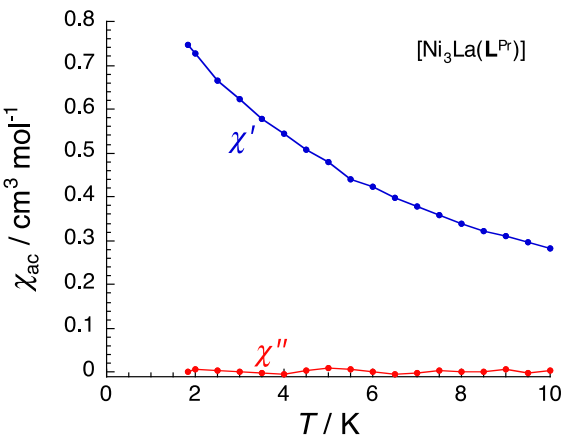

Figure S31. Temperature dependence below 10 K of the in- and out-of-phase components of ac susceptibility for $[Ni^{II}_3La^{III}(\mathbf{L^{Pr}})]$ at 1000 Hz with an amplitude of the ac field of 3 Oe.

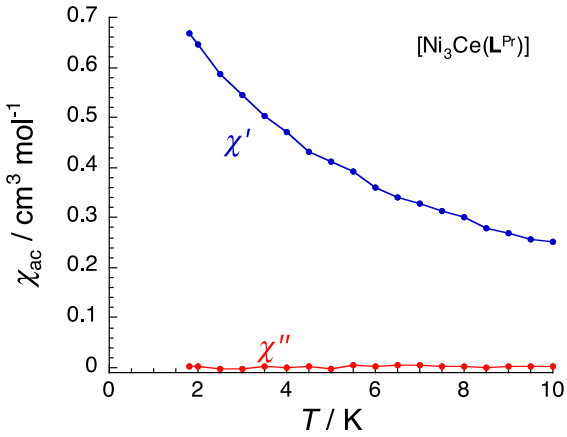

Figure S32. Temperature dependence below 10 K of the in- and out-of-phase components of ac susceptibility for $[Ni^{II}_3Ce^{III}(\mathbf{L^{Pr}})]$ at 1000 Hz with an amplitude of the ac field of 3 Oe.

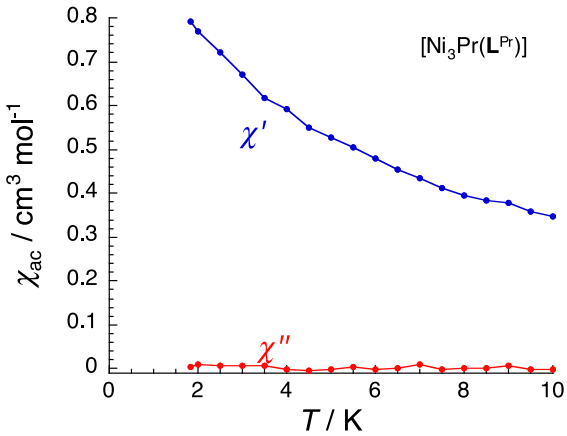

Figure S33. Temperature dependence below 10 K of the in- and out-of-phase components of ac susceptibility for $[Ni^{II}_3Pr^{III}(\mathbf{L^{Pr}})]$ at 1000 Hz with an amplitude of the ac field of 3 Oe.

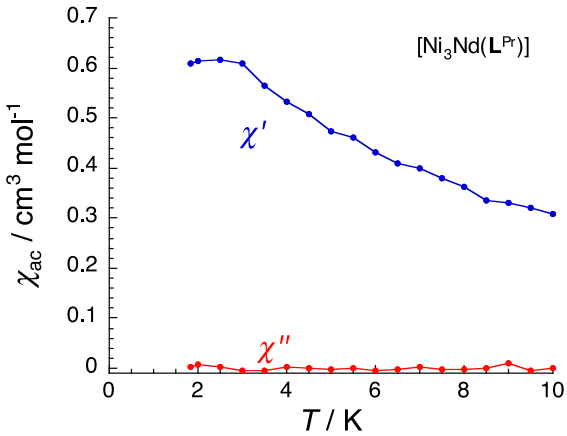

Figure S34. Temperature dependence below 10 K of the in- and out-of-phase components of ac susceptibility for $[Ni^{II}_3Nd^{III}(\mathbf{L^{Pr}})]$ at 1000 Hz with an amplitude of the ac field of 3 Oe.

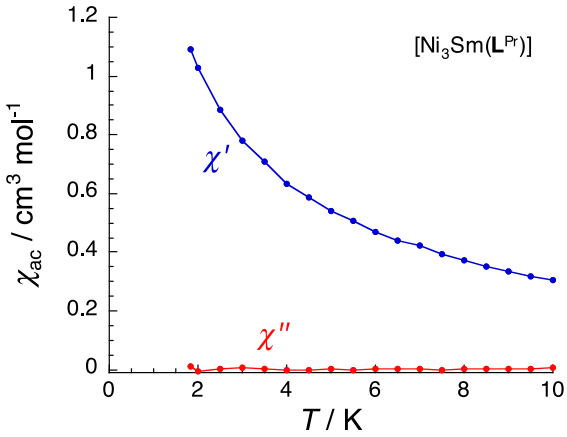

Figure S35. Temperature dependence below 10 K of the in- and out-of-phase components of ac susceptibility for $[Ni^{II}_3Sm^{III}(\mathbf{L^{Pr}})]$ at 1000 Hz with an amplitude of the ac field of 3 Oe.

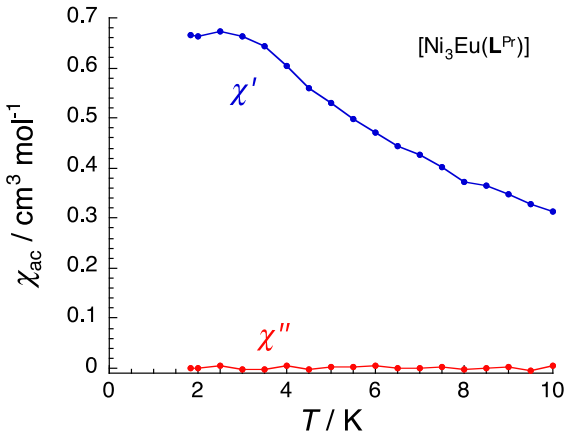

Figure S36. Temperature dependence below 10 K of the in- and out-of-phase components of ac susceptibility for $[Ni^{II}_3Eu^{III}(\mathbf{L^{Pr}})]$ at 1000 Hz with an amplitude of the ac field of 3 Oe.

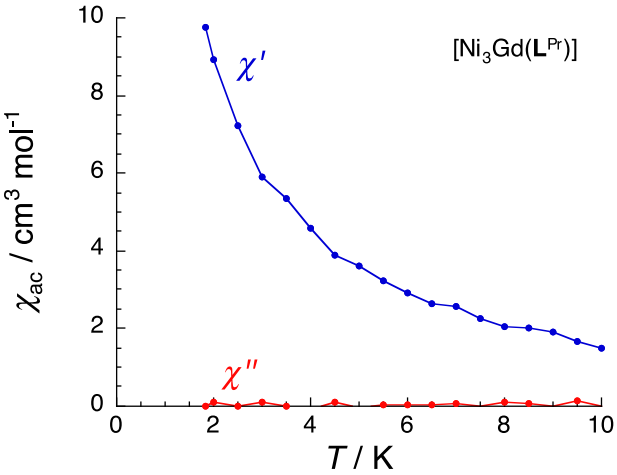

Figure S37. Temperature dependence below 10 K of the in- and out-of-phase components of ac susceptibility for $[Ni^{II}_3Gd^{III}(\mathbf{L^{Pr}})]$ at 1000 Hz with an amplitude of the ac field of 3 Oe.

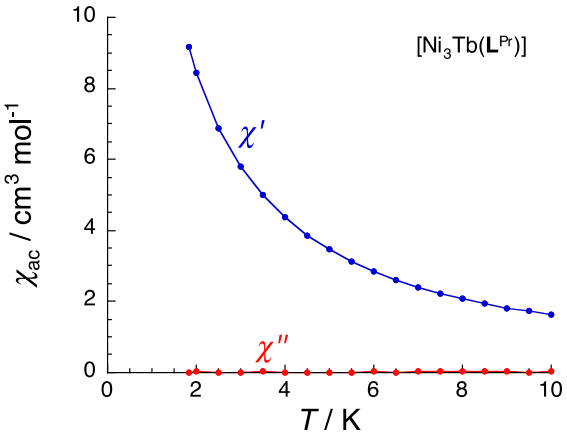

Figure S38. Temperature dependence below 10 K of the in- and out-of-phase components of ac susceptibility for $[Ni^{II}_3Tb^{III}(\mathbf{L^{Pr}})]$ at 1000 Hz with an amplitude of the ac field of 3 Oe.

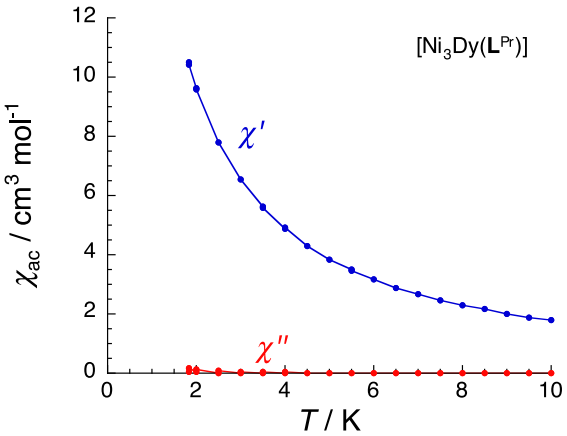

Figure S39. Temperature dependence below 10 K of the in- and out-of-phase components of ac susceptibility for $[Ni^{II}_3Dy^{III}(\mathbf{L^{Pr}})]$ at 1000 Hz with an amplitude of the ac field of 3 Oe.

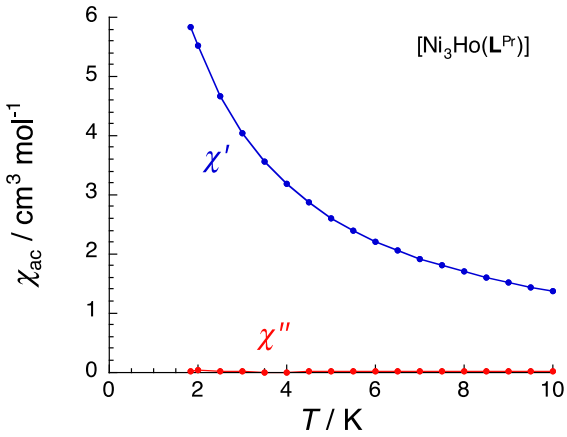

Figure S40. Temperature dependence below 10 K of the in- and out-of-phase components of ac susceptibility for $[Ni^{II}_3Ho^{III}(\mathbf{L^{Pr}})]$ at 1000 Hz with an amplitude of the ac field of 3 Oe.

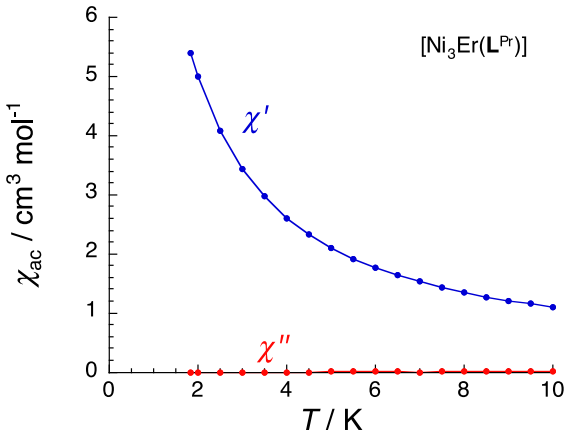

Figure S41. Temperature dependence below 10 K of the in- and out-of-phase components of ac susceptibility for $[Ni^{II}_3Er^{III}(\mathbf{L^{Pr}})]$ at 1000 Hz with an amplitude of the ac field of 3 Oe.

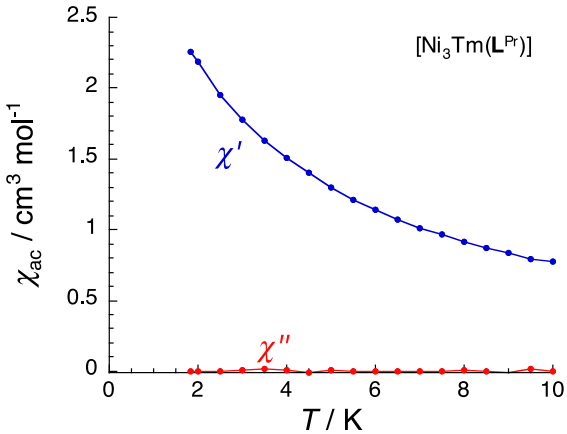

Figure S42. Temperature dependence below 10 K of the in- and out-of-phase components of ac susceptibility for $[Ni^{II}_3Tm^{III}(\mathbf{L^{Pr}})]$ at 1000 Hz with an amplitude of the ac field of 3 Oe.

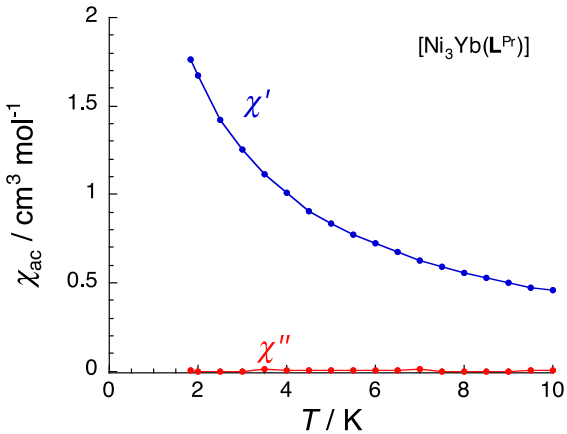

Figure S43. Temperature dependence below 10 K of the in- and out-of-phase components of ac susceptibility for $[Ni^{II}_3Yb^{III}(\mathbf{L^{Pr}})]$ at 1000 Hz with an amplitude of the ac field of 3 Oe.

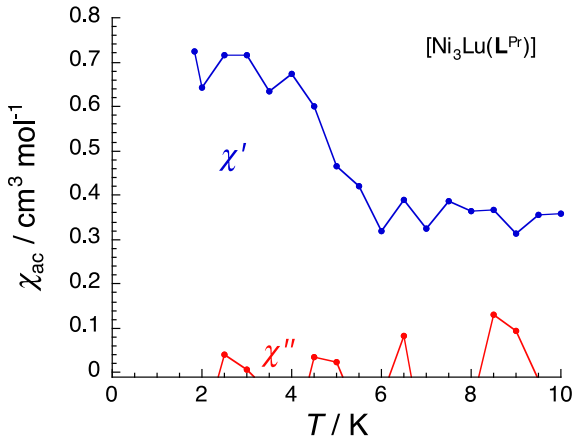

Figure S44. Temperature dependence below 10 K of the in- and out-of-phase components of ac susceptibility for $[Ni^{II}_3Lu^{III}(\mathbf{L^{Pr}})]$ at 1000 Hz with an amplitude of the ac field of 3 Oe.